ACS APPLIED MATERIALS & INTERFACES

Letter

www.acsami.org

Magnesium Anode for Chloride Ion Batteries

Xiangyu Zhao,[†,‡] Qiang Li,[‡] Zhirong Zhao-Karger,[‡] Ping Gao,[§] Karin Fink,[‡] Xiaodong Shen,[†] and Maximilian Fichtner*[,‡,§]

[†]College of Materials Science and Engineering, Nanjing Tech University, 5 Xinmofan Road, 210009 Nanjing, China

[‡]Institute of Nanotechnology, Karlsruhe Institute of Technology (KIT), Postfach 3640, 76021 Karlsruhe, Germany

[§]Helmholtz Institute Ulm (HIU) for Electrochemical Energy Storage, 89081 Ulm, Germany

Supporting Information

ABSTRACT: A key advantage of chloride ion battery (CIB) is its possibility to use abundant electrode materials that are different from those in Li ion batteries. Mg anode is presented as such a material for the first time and Mg/C composite prepared by ball milling of Mg and carbon black powders or thermally decomposed MgH_2/C composite has been tested as anode for CIB. The electrochemical performance of FeOCl/Mg and BiOCl/Mg was investigated, demonstrating the feasibility of using Mg as anode.

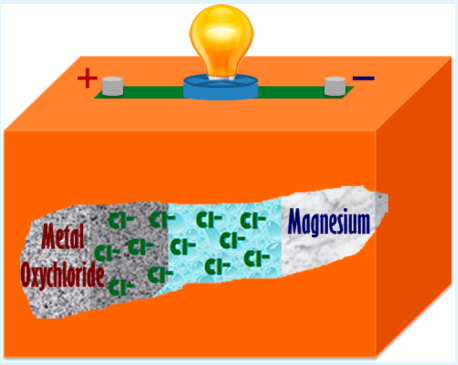

KEYWORDS: *chloride ion batteries, electrochemistry, magnesium anode, metal oxychlorides, ionic-liquid electrolytes*

The well-established lithium ion batteries play an increasingly important role in the field of energy storage because of their high energy densities.[1,2] Society's demand for electric vehicles and storing renewable energy such as solar and wind energy will require a large improvement in the energy density. Li−S and Li−O_2 batteries are receiving intense interest because of their potential to achieve a significant increase in capacity and reduction in cost of cathode materials.[3−6] Alternative battery chemistries using abundant anode materials such as Na or Mg have been developed, building new electrochemical systems based on Na^+ or Mg^{2+} as charge transfer ions.[7−10] Recently, the fluoride or chloride ion battery based on anion shuttle was reported.[11−14] The battery reactions can be expressed as follows

$$\text{Cathode: } M_cX_n + ne^- \leftrightarrow M_c + nX^- \quad (1)$$

$$\text{Anode: } M_a + mX^- \leftrightarrow M_aX_m + me^- \quad (2)$$

$$\text{Cell: } mM_cX_n + nM_a \leftrightarrow mM_c + nM_aX_m \quad (3)$$

where M_c is the metal in the cathode, M_a is the metal used in the anode, X is the halogen and m or n is the number of halide ions. This kind of battery uses a metal halide/metal electrochemical pair and lithium metal is not necessarily included. Both cathode and anode could be fabricated using sustainable materials. Moreover, a higher theoretical energy density than that of lithium ion batteries is offered. For instance, the chloride ion battery shows a theoretical energy density of up to 2500 Wh L^{-1}, which is close to that of Li−S battery.

However, a key hurdle caused by the dissolution of metal chloride cathodes in the ionic liquid electrolyte of chloride ion battery needs to be tackled for realizing a high energy density battery.[13] One approach is to use metal oxychlorides as cathode materials,[14] which are more stable than transition metal chlorides in the electrolyte. Then the overall reaction for chloride ion battery could be expressed as

$$mM_cOCl_n + nM_a \leftrightarrow mM_cO + nM_aCl_m \quad (4)$$

We previously investigated BiOCl/Li and FeOCl/Li electrode systems and proved the feasibility of using metal oxychlorides as cathode materials.[14] With respect to the above-mentioned goals, abundant magnesium would be a good choice for anode because of its low cost and two electrons redox reaction per molecule. In the following, we report the feasibility of using Mg as anode for chloride ion batteries by investigating the electrochemical performance of FeOCl/Mg and BiOCl/Mg electrochemical couples, by means of charge and discharge testing, cyclic voltammetry, X-ray diffraction, DFT + U + D2 calculations, and X-ray photoelectron spectroscopy.

We used magnesium foil (99.9%, 0.1 mm thick, Goodfellow) that was polished in the glovebox to remove the oxidation layer as the anode in the first experiments, but the battery did not discharge although a normal open circuit voltage (OCV) of the battery was measured. A second Mg anode that was prepared

Received: May 19, 2014
Accepted: July 7, 2014
Published: July 7, 2014

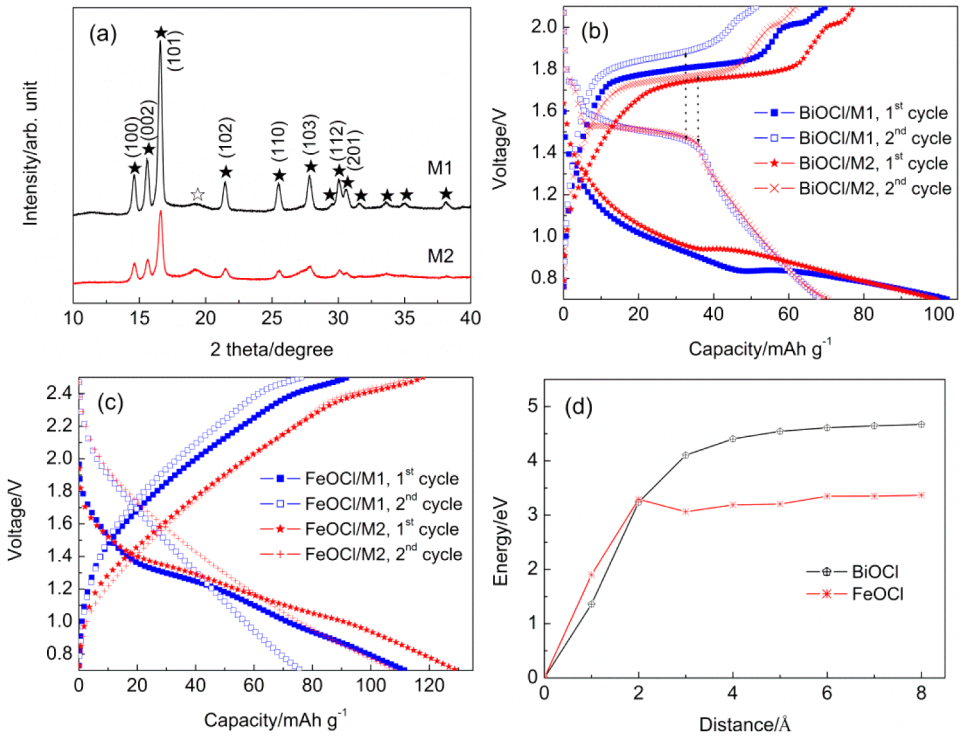

Figure 1. (a) XRD patterns of M1 and M2 composites. ★ Mg (PDF card no. 35−821); ☆ MgO (PDF card no.74−1225). M1, Mg/C composite prepared by ball milling of Mg and carbon black powders; M2, Mg/C composite prepared by thermal decomposition of MgH_2/C composite. (b, c) Discharge and charge curves of BiOCl/Mg (5 mA g^{-1}/0.048 *C*) and FeOCl/Mg (10 mA g^{-1}/0.04 *C*) full batteries using the electrolyte of 0.5 M $PP_{14}Cl$ in $PP_{14}TFSI$ at the first two cycles. (d) Simulated dissociation process of chloride ion from the surface of BiOCl and FeOCl by DFT + U + D2.

by a simple mixing of magnesium powder and carbon black in a mortar enabled discharge and charge of the metal oxychloride/Mg electrode system, stimulating the search for more active Mg anode composites. It was found that it is difficult to achieve a homogeneous elemental distribution of Mg in the composite because of the ductile magnesium, which would easily agglomerate during hard milling. Therefore, soft ball milling using light balls and low speed was carried out in order to avoid this unwanted effect. The product (M1) showed sharp diffraction peaks (Figure 1a), indicating a relatively large grain size. In this respect, it would be desirable to start with a suitable Mg precursor such as MgH_2 which is more brittle and does not agglomerate during ball milling. MgH_2/C composite was prepared by ball milling using tungsten carbide vial at a high speed. Then hydrogen desorption of the MgH_2/C composite was performed to obtain a more active Mg/C composite (M2), which showed much weaker and broader diffraction peaks than M1. For example, the average fwhm of the main peaks corresponding to (100), (002) and (101) planes of Mg increased from 0.28 to 0.33°, indicating a refinement of Mg grains.

Panels b and c in Figure 1 show the discharge and charge curves of BiOCl/Mg and FeOCl/Mg full batteries using the electrolyte of 0.5 M 1-butyl-1-methylpiperidinium chloride ($PP_{14}Cl$) in 1-butyl-1-methylpiperidinium bis-(trifluoromethylsulfonyl)imide ($PP_{14}TFSI$) in the following two cycles. Both electrode systems showed similar discharge and charge profiles when using Li as anode, i.e., a low discharge plateau in the first cycle, two redox reactions during cycling and sloping profiles for the electrode system using FeOCl as cathode.[14] The BiOCl cathode (BiOCl/M1) had an initial discharge capacity of 102 mAh g^{-1}, which is 99% the theoretical capacity (103 mAh g^{-1}). A charge capacity of 69 mAh g^{-1} was recovered in the first cycle, showing a Coulombic efficiency of 68%, while a higher Coulombic efficiency of 78% was obtained when M2 was used as anode. Moreover, the use of M2 anode contributed to a distinct decrease in the discharge/charge hysteresis, from 420 mV (M1) to 310 mV (M2), as shown in Figure 1b. The Coulombic efficiency of the BiOCl/M2 electrode system increased to 88% in the second cycle. The higher Coulombic efficiency indicated that M2 is more active. This facilitates the redox reaction at the anode side. For the FeOCl/Mg electrode system, similar results were obtained. The electrochemical polarization during charge was significantly decreased by using M2 and a Coulombic efficiency of 95% was achieved in the first cycle.

The discharge and charge curves present flat plateaus when using the BiOCl cathode, whereas sloping profiles were obtained for the FeOCl cathode, regardless of Li[14] or Mg anode. The flat plateau is attributed to the phase transformation between metal oxychoride and metal oxide. Our previous work demonstrated that BiOCl and FeOCl could lose chloride ion during discharge and transformed to metal oxides.[14] A probable explanation for the sloping profiles is the effect of nanosize of the active materials particles. The nanoscale particles have a large surface area, which can lead to a dominant surface reaction including a variety of energetic states, and thus a sloping profile.[15] The loss of chloride ion from FeOCl resulted in the formation of iron oxide with an ultrafine particle size of several nanometers, whereas a much larger size for bismuth oxide derived from the reduction of BiOCl.[14] Density-functional theory (DFT) calculations, with on-site Coulomb interaction (U) and dispersion (D2) corrections, based on the slab model (see Figure S1 in the Supporting Information) were

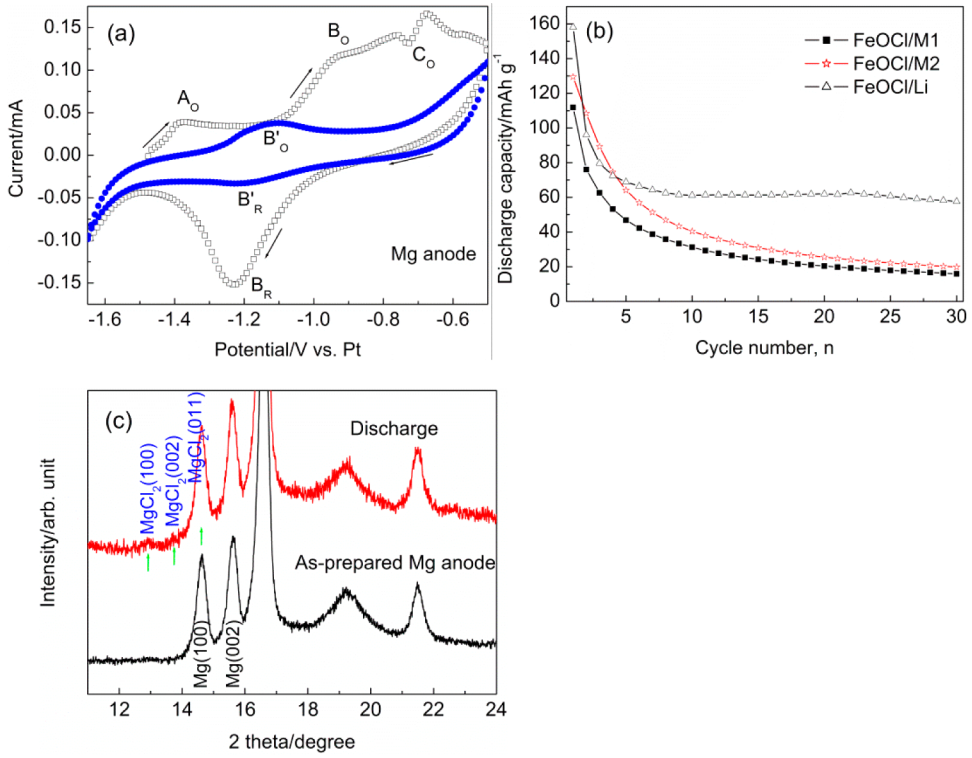

Figure 2. (a) CV patterns (1st and 2nd cycles, 60 μV s^{-1}) of Mg anode (see text). The counter electrode was FeOCl and the reference electrode was Pt. (b) Cycling performance of the FeOCl/Mg system, and (c) XRD patterns of Mg anode (FeOCl cathode, 7.5 mg; Mg anode: 14 mg) before and after discharge using the electrolyte of 0.5 M $PP_{14}Cl$ in $PP_{14}TFSI$ at 298 K. Mg, PDF card no. 35−821; $MgCl_2$, PDF card no. 72−1517.

performed to simulate the dissociation process of chloride ion from the surface of both BiOCl and FeOCl. The calculated energy barrier for the extraction of chloride ion in FeOCl is around 3.4 eV, which is much lower than ~4.7 eV for BiOCl, as shown in Figure 1d, indicating that the FeOCl showed a faster charge transfer reaction than BiOCl. Therefore, the sloping profiles of FeOCl may also be ascribed to its sluggish chloride ion diffusion in the bulk, which could not sustain the fast charge transfer reaction on the surface.

Figure 2a shows the CV patterns for Mg anode (M2) under the potential window from −1.65 to −0.5 V vs Pt. FeOCl cathode with higher discharge capacity and lower polarization than BiOCl cathode at the first cycle was chosen as the counter electrode. Three oxidation regions were observed at the first cycle. The small irreversible oxidation peak A_O is probably caused by the impurities in the electrolyte. Then the peak B_O may be attributed to the formation of $MgCl_2$ according to the XRD result in Figure 2c. The corresponding reduction peak is B_R. A large irreversible region C_O is likely due to the impurities in the electrolyte and/or partial decomposition of the electrolyte. In the second cycle, the C_O region disappeared. Only a pair of B_O' and B_R' peaks was observed, which may be ascribed to the redox reaction by the chloride ion transfer at the Mg anode side. The electrochemical polarization was reduced in the second cycle according to the decrease in the potential gap between the redox pair, from B_O/B_R to B_O'/B_R'.

Figure 2b shows the cycling performance of the FeOCl/Mg systems in the electrolyte of 0.5 M $PP_{14}Cl$ in $PP_{14}TFSI$ at 298 K. The FeOCl cathode has an initial discharge capacity of 111 mAh g^{-1} when using M1 as anode. The use of M2 with a higher activity contributed to an increase in the discharge capacity of FeOCl cathode to 130 mAh g^{-1}. Both FeOCl/Mg systems, however, showed capacity decay and their capacity retention rate after 30 cycles was only about 15%, which is much lower than that of the FeOCl/Li system. One reason for this capacity decay could be the large volume change of 197.5% from Mg to $MgCl_2$, leading to the interruption of electrical contact between partially active material and carbon black during cycling. For comparison, the volume change from Li to LiCl is only 56.5%. A better contact between active material and carbon needs to be achieved in the future work. Another reason may be the decomposition of the electrolyte at the surface of Mg anode mentioned above, which suppresses the chloride on transfer at the anode side. As the recent results of magnesium battery reported,[7,10,16] ether type of solvent has good compatibility with the Mg anode. This may be a choice for improving the electrochemical performance of chloride ion batteries based on Mg anode in the future work.

Figure 2c shows the XRD patterns of Mg anode before and after discharge. Weak diffraction peaks corresponding to (011), (002) and (100) planes of $MgCl_2$ were detected, demonstrating the chloride ion transfer from FeOCl cathode to Mg anode during discharge. The (011) peak of $MgCl_2$ is overlapped by the (100) peak of Mg according to the increase in the intensity ratio of (100) and (002) peaks of Mg from 88% to 92% after discharge. XPS was performed to further verify the structural evolution of Mg anode. We did not use any solvent to remove the residual electrolyte adsorbed on the surface of Mg anode during the ex-situ XPS test, since the solvent could also dissolve the $MgCl_2$ formed in the anode. Figure 3 shows the XPS region spectra of Cl 2p for Mg anode (FeOCl/Mg, M2) after cycling. Besides the peaks related to the chlorine in the electrolyte, new Cl 2p peaks were observed at higher binding energy position after discharge. The Cl $2p_{3/2}$ peak located at 199.7 eV was assigned to $MgCl_2$,[17] indicating the formation of $MgCl_2$ at the anode side after discharge, which is consistent with the XRD

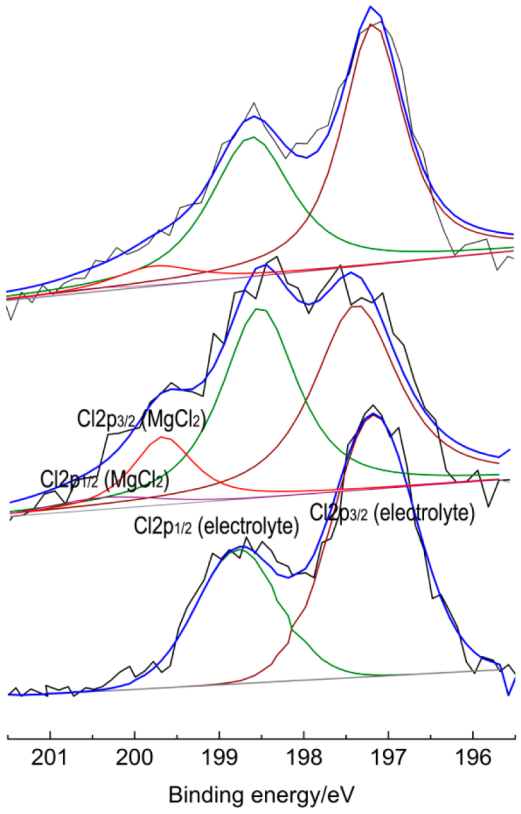

Figure 3. XPS region spectra of Cl 2p for Mg anode (FeOCl/Mg, M2) after cycling using the electrolyte of 0.5 M $PP_{14}Cl$ in $PP_{14}TFSI$ at 298 K. Bottom curves, electrolyte; middle, discharged Mg anode; top, recharged Mg anode.

result in Figure 2c. The intensity of the peak corresponding to $MgCl_2$ was significantly decreased after charge. This means the chloride ion was moved back from anode to cathode during charge, although part of $MgCl_2$ still remained at the anode side.

In summary, Mg/C composite prepared by ball milling of Mg and carbon black powders (M1) or thermally decomposed MgH_2/C composite (M2) was reported as anode in the FeOCl/Mg and BiOCl/Mg electrode systems. M2 composite showed a higher activity, and thus decreased the electrochemical polarization and increased the Coulombic efficiency. Discharge and charge testing, XRD and XPS results proved the chloride ion transfer at the Mg anode. However, the battery using Mg anode showed a large capacity decay during cycling, which may be attributed to the large volume change of Mg anode during chloride ion transfer and the decomposition of the electrolyte on the anode surface.

■ ASSOCIATED CONTENT

Ⓢ Supporting Information

Experimental details, including synthesis of materials, methods of calculation, and structural and electrochemical studies. This material is available free of charge via the Internet at http://pubs.acs.org.

■ AUTHOR INFORMATION

Corresponding Author

*E-mail: m.fichtner@kit.edu. Tel: +49 (0)721 608 25340. Fax: +49 (0)721 608 6368 (M.F.).

Author Contributions

The manuscript was written through contributions of all authors. All authors have given approval to the final version of the manuscript.

Notes

The authors declare no competing financial interest.

■ ACKNOWLEDGMENTS

X.Y.Z. acknowledges the support from the Priority Academic Program Development of Jiangsu Higher Education Institutions (PAPD).

■ REFERENCES

(1) Lee, J.; Urban, A.; Li, X.; Su, D.; Hautier, G.; Ceder, G. Unlocking the Potential of Cation-Disordered Oxides for Rechargeable Lithium Batteries. *Science* **2014**, *343*, 519−522.
(2) Goodenough, B.; Park, K. S. The Li-Ion Rechargeable Battery: A Perspective. *J. Am. Chem. Soc.* **2013**, *135*, 1167−1176.
(3) Yin, Y. X.; Xin, S.; Guo, Y. G.; Wan, L. J. Lithium−Sulfur Batteries: Electrochemistry, Materials, and Prospects. *Angew. Chem., Int. Ed.* **2013**, *52*, 13186−13200.
(4) Evers, S.; Nazar, L. F. New Approaches for High Energy Density Lithium-Sulfur Battery Cathode. *Acc. Chem. Res.* **2012**, *46*, 1135−1143.
(5) Bruce, P. G.; Freunberger, S. A.; Hardwick, L. J.; Tarascon, J. M. Li-O_2 and Li-S Batteries with High Energy Storage. *Nat. Mater.* **2012**, *11*, 19−29.
(6) Zhang, T.; Zhou, H. S. A Reversible Long-Life Lithium-Air Battery in Ambient Air. *Nat. Commun.* **2013**, *4*, 1817.
(7) Yoo, H. D.; Shterenberg, I.; Gofer, Y.; Gershinsky, G.; Pour, N.; Aurbach, D. Mg Rechargeable Batteries: An On-Going Challenge. *Energy Environ. Sci.* **2013**, *6*, 2265−2279.
(8) Wang, R. Y.; Wessells, C. D.; Huggins, R. A.; Cui, Y. Highly Reversible Open Framework Nanoscale Electrodes for Divalent Ion Batteris. *Nano Lett.* **2013**, *13*, 5748−5752.
(9) Mohtadi, R.; Matsui, M.; Arthur, T. S.; Hwang, S. J. Magnesium Borohydride: From Hydrogen Storage to Magnesium Battery. *Angew. Chem., Int. Ed.* **2012**, *51*, 9780−9783.
(10) Saha, P.; Datta, M. K.; Velikokhatnyi, O. I.; Manivannan, A.; Alman, D.; Kumta, P. N. Rechargeable Magnesium Battery: Current Status and Key Challenges for the Future. *Prog. Mater. Sci.* **2014**, *66*, 1−86.
(11) Anji Reddy, M.; Fichtner, M. Batteries Based on Fluoride Shuttle. *J. Mater. Chem.* **2011**, *21*, 17059−17062.
(12) Rongeat, C.; Anji Reddy, M.; Witter, R.; Fichtner, M. Solid Electrolytes for Fluoride Ion Batteries: Ionic Conductivity in Polycrystalline Tysonite-Type Fluorides. *ACS Appl. Mater. Interfaces* **2014**, *6*, 2103−2110.
(13) Zhao, X. Y.; Ren, S.; Bruns, M.; Fichtner, M. Chloride Ion Battery: A New Member in The Rechargeable Battery Family. *J. Power Sources* **2014**, *245*, 706−711.
(14) Zhao, X. Y.; Zhao-Karger, Z.; Wang, D.; Fichtner, M. Metal Oxychlorides as Cathode Materials for Chloride Ion Batteries. *Angew. Chem., Int. Ed.* **2013**, *52*, 13621−13624.
(15) Devaraju, M. K.; Tomai, T.; Unemoto, A.; Honma, I. Novel Processing of Lithium Manganese Silicate Nanomaterials for Li-ion Battery Applications. *RSC Adv.* **2013**, *3*, 608−615.
(16) Muldoon, J.; Bucur, C. B.; Oliver, A. G.; Sugimoto, T.; Matsui, M.; Kim, H. S.; Allred, G. D.; Zajicek, J.; Kotani, Y. Electrolyte Roadblocks to a Magnesium Rechargeable Battery. *Energy Environ. Sci.* **2012**, *5*, 5941−5950.
(17) Karakalos, S.; Siokou, A.; Ladas, S. The Interfacial Properties of $MgCl_2$ Films Grown on a Flat SiO_2/Si Substrate. An XPS and ISS Study. *Appl. Surf. Sci.* **2009**, *255*, 8941−8946.